Monte Carlo Calculations for a Fusion Reactor Blanket and Shield

L.A. El-Guebaly and C.W. Maynard

January 1974

UWFDM-79

Trans. ANS 18, 25 (1974).

FUSION TECHNOLOGY INSTITUTE

UNIVERSITY OF WISCONSIN

MADISON WISCONSIN

Monte Carlo Calculations for a Fusion Reactor Blanket and Shield

L.A. El-Guebaly and C.W. Maynard

Fusion Technology Institute
University of Wisconsin
1500 Engineering Drive
Madison, WI 53706

http://fti.neep.wisc.edu

January 1974

UWFDM-79

Trans. ANS 18, 25 (1974).

Monte Carlo Calculations for a Fusion Reactor Blanket and Shield

by

L. A. El-Guebaly and C. W. Maynard

January 1974

FDM 79

University of Wisconsin

I. Introduction

In fusion neutronics calculations, there is a need for a calculational method that is capable of determining the neutron flux for a three dimentional design with an arbitrary geometrical configuration. Usually, one is forced to rely on the Monte Carlo method, especially when the reactor geometry is complicated.

The neutronics calculations for the blanket and shield in the present study, were performed using the Monte Carlo program MORSE[1,2]. The proper operation of the program is checked against the flux calculations of the standard blanket fusion reactor model[3] using the transport code ANISN[4] which employs the same cross section data sets as MORSE. All data used for the performed calculations were taken from the ENDF/B files.

Section II of this paper is focused directly on the standard blanket calculations. Section III is devoted to the neutronics calculations of the unit cell and blanket and shield assembly of the Austin design. The neutronics calculations of the UWMAK-I is the subject of section IV. A conclusion from this study is presented in Section V. The final section deals with the corrections which have been made to the MORSE program.

II. Standard Blanket

In order to check the proper operation of the MORSE code, the standard blanket model shown in Figure 1 was considered as a sample problem. The problem was run with 35 energy groups and P_3 anisotropic scattering cross sections. An isotropic source of 14.1 MeV neutrons uniformly distributed throughout a central cylinder of 150 cm radius was employed and 1000 histories were followed. A geometry of infinitely long concentric cylinders was considered for the blanket and an outside vacuum boundary condition was assumed. A normalization factor of 4.43×10^{14} n/cm^2/sec on the first wall was used.

The flux distribution versus region number from MORSE is shown in Figure 2, while the flux distribution versus interval number from ANISN is shown in Figure 3. In general, both calculations are in good agreement within the statistical error of the MORSE results.

III. Austin Design

The fusion reactor design shown in Figure 4 is represented for neutronics calculations by the blanket and shield assembly shown in Figure 5.

A. The Unit Cell

The blanket is composed of a large number of unit cells to moderate neutrons, breed tritium, and remove heat[5]. A schematic view of the unit cell is shown in Figure 6.

The purpose of carrying out Monte Carlo calculations for the unit cell, is to study the effect of the first wall curvature and homogenization on the flux distribution. Two problems based on the possible representations of the first wall, have been considered. In the first problem, the first wall has a cylindrical shape which is the actual case. In the second problem, the first wall is considered as a slab (Figure 7) with the same amount of material as the former case. The latter case has been used, with a homogeneous medium of regions I, II, VI and VII, for a discrete ordinates calculation for the blanket.

For each problem, the histories of 1000 source neutrons were followed, 46 energy groups (Table I), and P_3 scattering anisotropy were used, and vacuum boundary conditions were assumed outside region X. The flux distributions in the different regions are summarized in

Table II. The results in all regions are in good agreement within the statistical error. Only in region X is the discrepancy between the two cases slightly larger than the statistical error and it is expected that can be removed by running more histories. The first wall flux is slightly lower in Case 1. This results from the fact that the thinner areas of a wall of variable projected thickness transmit more particles than are stopped by extra material in the thicker areas.

The flux spectrum in regions I, II and V are shown in Figures 8, 9, and 10 respectively. The solid lines represent case 1 and the dashed lines represent case 2. Figure 10 shows that in case 2 the high flux is primarily due to neutrons having energies slightly lower than the source energy as a result of the extra thermalization of the source neutrons by the thicker first wall. That leads to a slight decrease in the high energy neutrons, which produce $Li^7(n,n'T)\alpha$ reactions in regions I and II as shown in Figures 8 and 9 respectively. This reduction yields a low tritium production from Li^7 in case 2.

The tritium production for cases 1 and 2 are listed in Table III. Comparing with ANISN[6], one finds good agreement between the three results within the statistical error.

A major conclusion which emerges from the unit cell results is that slab geometry is a good representation for the first wall from the neutronics point of view. Thus, to reduce the computation cost, the neutronics calculations for the unit cell of new designs can be performed by the discrete ordinates method without introducing appreciable error to the results.

B - The Blanket and Shield Calculations

The blanket and shield assembly shown in Figure 5 is infinitely long in the direction perpendicular to the page. Due to problem symmetry about the horizontal mid plane, only the upper half of the blanket and shield were considered with an albedo reflecting boundary at the mid plane. Homogenized mixtures for the blanket and shield are based on the composition of the unit cell (Figure 6) and shield. Schematic representation of the shield is shown in Figure 11.

The main purpose in carrying out these calculations has been to study: 1) the effect of source representation on the flux distribution, 2) the effect of the divertor slots on tritium breeding, and 3) the leakage of neutrons through the divertor slots.

Throughout the calculations, 46 neutron energy groups and P_3 scattering anisotropy have been used. The histories of 4000 source neutrons were followed and vacuum boundary conditions were assumed outside the shield.

The plasma is considered as an isotropic source of 14.1 MeV neutrons. Three different source representations were chosen based on combinations between plasma spatial shapes and density distributions:

1) Actual plasma shape with uniform density distribution

2) Circular plasma shape with uniform density distribution

3) Circular plasma shape with parabolic density distribution.

The flux distributions for the three cases are given in Table IV. The leakage probability from the slots as well as from the boundaries of the shield are given in Table V. Tritium production from $Li^7(n,n'T)\alpha$ and $Li^6(n,T)\alpha$ reactions, by region, are summarized

in Table VI (reaction rates are normalized to one source neutron). The flux per unit energy is plotted versus energy for blanket and first wall regions (Figures 12 to 18) for the three cases.

The results for the flux distribution in the three cases are generally in good agreement within the statistical error. This means that the results do not depend to a great extent on the source distribution and a simple representation of the source is adequate for our calculations.

In general, the flux spectrum in the blanket and first wall regions are in good agreement for the three cases, and only in some of the low energy groups are there slight discrepancies.

Table VI shows the agreement (within statistical error) in the reaction rates for the three cases. The tritium breeding is not sensitive to the source representation and, even in the presence of the slots, it is more than adequate. Comparing with discrete ordinate calculations,[6] one will find discrepancies of up to 9% with a lower breeding ratio obtained in the Monte Carlo calculations. These discrepancies are due to differences in the calculated $Li^7(n,n'T)\alpha$ reaction rates which are induced by high energy neutrons. In Monte Carlo calculations, a homogenous mixture is used in the blanket. The uniformly distributed graphite in this case softens the spectrum considerably and a reduced $Li^7(n,n'T)\alpha$ reaction rate results.

The leakage from the slots is higher in case 1 than in cases 2 and 3 as would be expected. Almost all escapes from the slots occur from slot 1 and only a very few low energy neutrons escape from slot 2. It is concluded that neutron escape from the slots is small and a few centimeters of stainless steel suffices to protect the regions behind them.

IV. UWMAK-I Blanket and Shield Calculations

In order to study the leakage of neutrons from the vacuum openings, the UWMAK-I blanket and shield have been represented for neutronics calculations by the configuration shown in Figure 19. An albedo reflecting boundary is placed at the mid plane while vacuum boundary conditions are considered outside the shield. The height of the system is based on a unit of the twelve sectors of the torus which contains one vacuum opening.

The calculations have been carried out with 46 energy groups, P_3 scattering anisotropy and histories of 4000 source neutrons uniformly distributed throughout the actual plasma shape. Homogenized mixtures for the shield and blanket are used. Schematic representations are shown in Figure 20 for the shield and the blanket on both sides of the plasma.

The results for the flux distribution in the various regions as well as the tritium production in the blanket, are summarized in Table VII. The leakage probability and energy leakage from the vacuum opening are found to be 0.3635% and 0.2376×10^{-3} Mev/Mev respectively, while the leakage probability from the shield boundaries is 0.2115%.

In conclusion, the leakage of the neutrons from the vacuum openings is negligible and the part of the blanket represented by region X provides good protection.

V. Conclusion

It is useful to summarize in several points the results of the Monte Carlo calculations for the Univ. of Wisconsin fusion reactor blanket and shield:

1.) A simple representation of the neutron source is adequate for the neutronics calculations.

2.) The flux spectrum in the different regions is not sensitive to the source representation. As a result, any reaction rate with a certain source distribution can be calculated using the flux spectrum of another source distribution with no need of repeating the calculations and without introducing appreciable error to the results.

3.) The slots have no effect on the tritium breeding.

4.) a) The neutron leakage from any well protected opening is very small and can be neglected.

b) A few centimeters of structural material suffices to protect the regions behind any opening.

VI. Corrections to MORSE Code

Subroutine	Statement Number	Changes	Comments
CPUTM	-2,2	MICS = URTIMF (DUM)*1000	
ENDRUN	-99	IF (NREG.EQ.---) GØ TØ 86	Exclude regions which contain media with
	-106	GØ TØ 90	no stored cross sections (e.g. internal
		86 WTS(L) = 0.0	void, external void, and albedo medium).
	-113	IF (NREG.EQ.---) GØ TØ 101	
	-120	GØ TØ 105	
		101 WTS(L) = 0.0	
	-135,135	Eliminate the last right parenthesis on this line.	
GENI	-106,106	GØ TØ 221	In the MA array, assign the input zone
		220 IALP = IR1	number to the corresponding code zones.
GG	-42,42 C	221 DØ 230 I = k,9	
	-52	IF(DZ.LT.0.) GØ TØ 1121	For the ARB, if RIN is -ve and RØUT is +ve
	-55	IF(RIN.LT.0.) GØ TØ 2000	the particle is inside the body.
	-63	1121 IF(RIN.LT.0.) GØ TØ 1122	
		RIN = DZ	
		LRI = L	
		IF (RØUT.GT.0.) GØ TØ 2000	
		GØ TØ 1190	
		1122 IF(RIN.GE.DZ) GØ TØ 1123	
		RØUT = DZ	
		LRØ = L	
		GØ TØ 2000	
		1123 RØUT = RIN	
		LRØ = LRI	
		RIN = DZ	
		LRI = L	
		GØ TØ 2000	
GØMST	-61,61	CALL NØRML (NSTØR(KMA),	Call Subroutine NØRML if there is any
		.NSTØR (KFPD),NSTØR(KLCR),NSTØR(KNBD),	albedo scattering. Note that it is
		.NSTØR (KKR1),NSTØR(KKR2))	called from GØMST and not from ALBDO
		IRPRIM = IR	as it is stated in the manual[2].
		BLZNT = IRPRIM	
		NASC = -1	
GTMED	-2,2	MDXSEC = MDGEØM	Set cross section medium same as Geometry medium.

(cont.)

Subroutine	Statement Number	Changes	Comments
INPUT1	-565,565	LAL = NSTØR(NGEØM) CALL JØMIN(LAL,I1,IO) NSTØR(NGEØM) = LAL	
INSCØR	-12	DIMENSIØN VØLM(MXREG)	Store the reciprocal of the volume for the
		DATA VØLM/--,--,-----,--/	corresponding detector region (the volumes
	-20,28	5 BC(LF)= 1./VØLM(ID-NDC)	of the different regions have to be entered
NØRML	-1,1	SUBRØUTINE NØRML(MA,FPD,LOCREG,	in the data statement.)
		.NUMBØD, IR1,IR2)	
		DIMENSIØN IR1(1),IR2(1)	
	-5,5	.KKR1, KKR2,KNSR,KVØL,NADD,LDATA,	
		.LTMA, LFPD,NUMR,IRTRU,NUMB,NIR	
	-21,25	JR1 = IR1(IR)	
		JR2 = IR2(IR)	Return the correct normal to the surface
		DØ 40 IRR = JR1,JR2	in case of more code zones than input zones.
		N = LØCREG(IRR) + 1	
		NUM = NUMBØD(IRR)*4+N-4	
		DØ 40 I = N, NUM, 4	
		IF(NASC.EQ.IABS(MA(I)))GØ TØ 100	
		40 CONTINUE	
NSIGTA	-17	IF(MED.EQ.1000.ØR.MED.EQ.0)GØ TØ 11	Exclude the computation of TSIG and
	-41,41	GØ TØ 12	PNAB in case of internal and external
		11 TSIG = 0.	voids
		PNAB = 0.	
		12 RETURN	
RELCØL	-15,16	C	
	-18,28	CØN = WTBC/TSIG	A detector number from NDC + 1 to ND is
		ID = NREG + NDC	chosen depending on the value of NREG.

References

1. Straker, E. A., et.al., "The MORSE Code - A Multigroup Neutron and Gamma Ray Monte Carlo Transport Code," ORNL-4585, Oak Ridge National Laboratory (1970).

2. Straker, E. A., et. al., "The MORSE Code with Combinatorial Geometry," SAI-72-511-LJ (1972).

3. S. Blow, "Standard Model for Comparison of Neutronics Codes," Oak Ridge, Tennessee,(1971).

4. W. Engle, A User Manual for ANISN, A one Dimensional Discrete Ordinates Transport Code with Anisotropic Scattering, Report 1693, Oak Ridge, Tenn. (1967).

5. D. Sze and w. Stewart, "Lithium Cooling For a low - β Tokamak Reactor", University of Wisconsin FDM-32,(Nov. 1972).

6. University of Wisconsin Study Team, "Preliminary Conceptual Design of a Tokamak Reactor," University of Wisconsin FDM-36, (Nov. 1972).

Table I

Neutron 46 Energy Group Structure in ev

Group	Group Limits E(Top)	E(Low)	E(Mid Point)
1	1.4918 (+7)*	1.3499 (+7)	1.4208 (+7)
2	1.3499 (+7)	1.2214 (+7)	1.2856 (+7)
3	1.2214 (+7)	1.1052 (+7)	1.1633 (+7)
4	1.1052 (+7)	1.0000 (+7)	1.0526 (+7)
5	1.0000 (+7)	9.0484 (+6)	9.5242 (+6)
6	9.0484 (+6)	8.1873 (+6)	8.6178 (+6)
7	8.1873 (+6)	7.4082 (+6)	7.7979 (+6)
8	7.4082 (+6)	6.7032 (+6)	7.0557 (+6)
9	6.7032 (+6)	6.0653 (+6)	6.3843 (+6)
10	6.0653 (+6)	5.4881 (+6)	5.7787 (+6)
11	5.4881 (+6)	4.9659 (+6)	5.2270 (+6)
12	4.9659 (+6)	4.4933 (+6)	4.7296 (+6)
13	4.4933 (+6)	4.0657 (+6)	4.2795 (+6)
14	4.0657 (+6)	3.6788 (+6)	3.8722 (+6)
15	3.6788 (+6)	3.3287 (+6)	3.5038 (+6)
16	3.3287 (+6)	3.0119 (+6)	3.1703 (+6)
17	3.0119 (+6)	2.7253 (+6)	2.8686 (+6)
18	2.7253 (+6)	2.4660 (+6)	2.5956 (+6)
19	2.4660 (+6)	1.8268 (+6)	2.1251 (+6)
20	1.8268 (+6)	1.3534 (+6)	1.5743 (+6)
21	1.3534 (+6)	1.0026 (+6)	1.1663 (+6)
22	1.0026 (+6)	7.4274 (+5)	8.6401 (+5)
23	7.4274 (+5)	5.5023 (+5)	6.4008 (+5)
24	5.5023 (+5)	4.0762 (+5)	4.7418 (+5)
25	4.0762 (+5)	3.0197 (+5)	3.5128 (+5)
26	3.0917 (+5)	2.2371 (+5)	2.6024 (+5)
27	2.2371 (+5)	1.6573 (+5)	1.9279 (+5)
28	1.6573 (+5)	1.2277 (+5)	1.4282 (+5)
29	1.2277 (+5)	6.7379 (+4)	9.8803 (+4)
30	6.7379 (+4)	3.1828 (+4)	4.6671 (+4)

Table I (continued)

Group	Group Limits E(Top)	E(Low)	E(Mid Point)
31	3.1828 (+4)	1.5034 (+4)	2.2046 (+4)
32	1.5034 (+4)	7.1017 (+3)	1.0414 (+4)
33	7.1017 (+3)	3.3546 (+3)	4.9191 (+3)
34	3.3546 (+3)	1.5846 (+3)	2.3236 (+3)
35	1.5846 (+3)	7.4852 (+2)	1.0976 (+3)
36	7.4852 (+2)	3.5358 (+2)	5.1847 (+2)
37	3.5358 (+2)	1.6702 (+2)	2.4491 (+2)
38	1.6702 (+2)	7.8893 (+1)	1.1569 (+2)
39	7.8893 (+1)	3.7267 (+1)	5.4647 (+1)
40	3.7267 (+1)	1.7603 (+1)	2.5813 (+1)
41	1.7603 (+1)	8.3153 (+0)	1.2193 (+1)
42	8.3153 (+0)	3.9279 (+0)	5.7597 (+0)
43	3.9279 (+0)	1.8554 (+0)	2.7207 (+0)
44	1.8554 (+0)	8.7643 (-1)	1.2852 (+0)
45	8.7643 (-1)	4.1399 (-1)	6.0707 (-1)
46	4.1399 (-1)	2.200 (-2)	2.1800 (-1)

* ($\pm$ n) represents ($10^{\pm n}$)

Table II

Flux Distribution

Case / Region	1	2
1	$1.3165 \pm .0148$	$1.3268 \pm .0193$
2	$2.4945 \pm .0793$	$2.6137 \pm .0876$
3	$(5.3874 \pm .228)10^{-1}$	$(4.5662 \pm .23)10^{-1}$
4	$(5.4497 \pm .665)10^{-2}$	$(6.1263 \pm .65)10^{-2}$
5	$2.8606 \pm .138$	$3.0198 \pm .131$
6	$1.2968 \pm .0367$	$1.3245 \pm .0289$
7	$1.3017 \pm .0308$	$1.3102 \pm .027$
8	$(7.8974 \pm .427)10^{-1}$	$(7.3825 \pm .378)10^{-1}$
9	$(1.5367 \pm .244)10^{-1}$	$(1.2462 \pm .2068)10^{-1}$
10	$(2.3535 \pm .459)10^{-2}$	$(1.2471 \pm .346)10^{-2}$

Table III

Tritium Production

Case	Curved 1st Wall		Straight 1st Wall	
Region \ T	T_7	T_6	T_7	T_6
1	.3955 ± .01536	.8693 ± .01129	.3585 ± .01278	.8719 ± .0112
2	.08615 ± .004552	.05014 ± .001693	.07896 ± .005536	.05425 ± .00233
4	.003275 ± .001622	.1065 ± .008144	.006818 ± .002424	.1111 ± .009036
Total	0.48494 ± .0161	1.026 ± .014	0.44427 ± .0141	1.0372 ± .0145
$T_6 + T_7$	1.51094 ± .02135		1.48147 ± .02031	

Table IV

Flux Distribution

Region	Case 1	Case 2	Case 3
1	$(2.8414 \pm .0834) \times 10^{-7}$	$(2.8791 \pm .0590) \times 10^{-7}$	$(2.8736 \pm .0659) \times 10^{-7}$
2	$(3.4624 \pm .0855) \times 10^{-7}$	$(3.3525 \pm .0728) \times 10^{-7}$	$(3.4499 \pm .0529) \times 10^{-7}$
3	$(1.8359 \pm .0813) \times 10^{-7}$	$(1.7866 \pm .0711) \times 10^{-7}$	$(1.8319 \pm .0924) \times 10^{-7}$
4	$(3.2047 \pm .0649) \times 10^{-7}$	$(3.2513 \pm .0709) \times 10^{-7}$	$(3.1890 \pm .0738) \times 10^{-7}$
5	$(1.3723 \pm .2192) \times 10^{-9}$	$(2.010 \pm .2935) \times 10^{-9}$	$(1.7795 \pm .2328) \times 10^{-9}$
6	$(4.4195 \pm .5606) \times 10^{-9}$	$(3.3977 \pm .4294) \times 10^{-9}$	$(3.9859 \pm .6803) \times 10^{-9}$
7	$(3.4036 \pm .5117) \times 10^{-9}$	$(2.4764 \pm .4076) \times 10^{-9}$	$(3.5645 \pm .5428) \times 10^{-9}$
8	$(1.9801 \pm .3968) \times 10^{-8}$	$(2.1283 \pm .5150) \times 10^{-8}$	$(1.9102 \pm .3778) \times 10^{-8}$
9	$(3.5961 \pm .4345) \times 10^{-9}$	$(3.3218 \pm .3705) \times 10^{-9}$	$(3.3485 \pm .3550) \times 10^{-9}$
10	$(1.3591 \pm .1744) \times 10^{-6}$	$(1.1478 \pm .0439) \times 10^{-6}$	$(1.2254 \pm .0910) \times 10^{-6}$
11	$(1.1736 \pm .0358) \times 10^{-6}$	$(1.1956 \pm .0323) \times 10^{-6}$	$(1.1974 \pm .0339) \times 10^{-6}$
12	$(1.1344 \pm .0360) \times 10^{-6}$	$(1.1950 \pm .0620) \times 10^{-6}$	$(1.1994 \pm .0977) \times 10^{-6}$

Table V

Summary of Leakage Probabilities

Leakage \ case	1	2	3
Leakage Prob. from slots	0.248%	0.222%	0.231%
Energy Leakage from slots (Mev/Mev)	0.325×10^{-3}	0.186×10^{-3}	0.145×10^{-3}
Leakage prob. from the shield boundaries	0.234%	0.151%	0.172%

Table VI

Tritium Production

Case	Case 1		Case 2		Case 3	
T / Region	T_7	T_6	T_7	T_6	T_7	T_6
1	.1385 ± .0072	.2953 ± .0073	0.1374 ± .0041	0.3037 ± .0064	0.1357 ± .0043	0.2985 ± .0069
2	.1354 ± .0051	.2963 ± .0067	0.1322 ± .0043	0.2880 ± .0060	0.1391 ± .0042	0.2908 ± .0048
3	.0276 ± .0020	.0718 ± .0033	0.0298 ± .0018	0.0669 ± .0031	0.0321 ± .0028	0.0684 ± .0033
4	.1226 ± .0049	.2731 ± .0055	0.1288 ± .0041	0.2792 ± .0062	0.1268 ± .0045	0.2782 ± .0062
Total	.4241 ± .0103	.9365 ± .0118	0.4282 ± .0074	0.9378 ± .0111	0.4337 ± .0080	0.9359 ± .0110
$T_7 + T_6$	1.3606 ± .0157		1.3660 ± 0.0134		1.3696 ± 0.0136	

Table VII

Flux Distribution and Tritium Production

Region	Flux Distribution	Tritium Production	
		T_7	T_6
1	$(6.2459 \pm .3074) \times 10^{-7}$	---	---
2	$(5.6657 \pm .2589) \times 10^{-7}$	---	---
3	$(5.2111 \pm .4841) \times 10^{-7}$	---	---
4	$(5.1676 \pm .3379) \times 10^{-7}$	---	---
5	$(4.2472 \pm .1895) \times 10^{-7}$	---	---
6	$(5.4715 \pm .2508) \times 10^{-7}$	---	---
7	$(2.4221 \pm .0903) \times 10^{-7}$	$.07463 \pm .00539$	$.2164 \pm .0067$
8	$(2.2797 \pm .0512) \times 10^{-7}$	$.06184 \pm .00287$	$.2090 \pm .0048$
9	$(1.8053 \pm .0935) \times 10^{-7}$	$.02882 \pm .00240$	$.1000 \pm .0053$
10	$(2.5486 \pm .0833) \times 10^{-7}$	$.02103 \pm .00130$	$.0847 \pm .0022$
11	$(1.4320 \pm .0550) \times 10^{-7}$	$.03511 \pm .00273$	$.1272 \pm .0047$
12	$(1.7801 \pm .0530) \times 10^{-7}$	$.07373 \pm .00324$	$.2072 \pm .0066$
13	$(1.4845 \pm .2449) \times 10^{-8}$	---	---
14	$(1.2874 \pm .1460) \times 10^{-8}$	---	---
15	$(1.4504 \pm .1345) \times 10^{-8}$	---	---
16	$(6.1927 \pm .9480) \times 10^{-9}$	---	---

Total = $1.23967 \pm .01511$

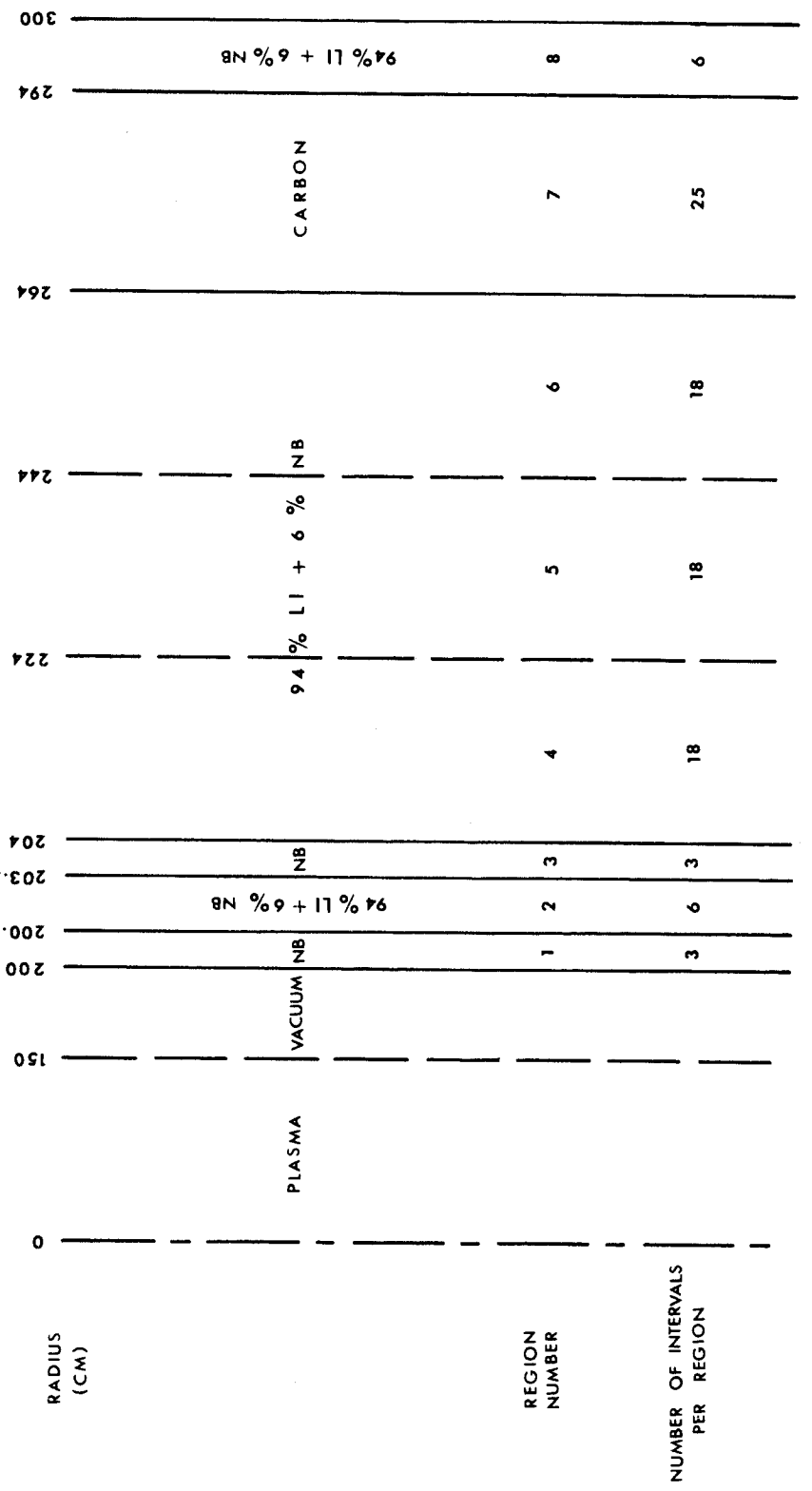

FIG.1 SCHEMATIC OF STANDARD BLANKET

FIG.2- FLUX DISTRIBUTION - MORSE

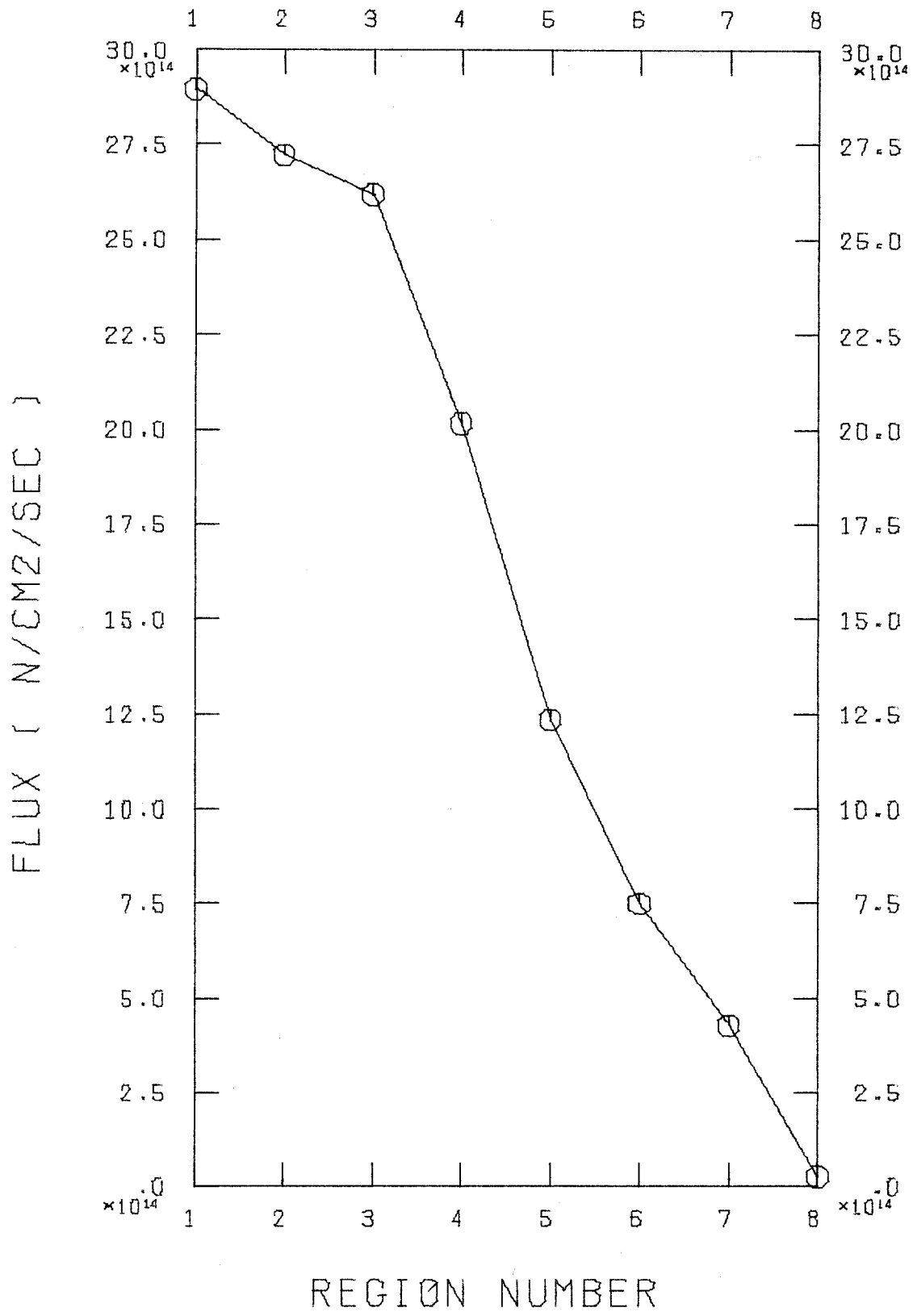

FIG.3- FLUX DISTRIBUTION - ANISN

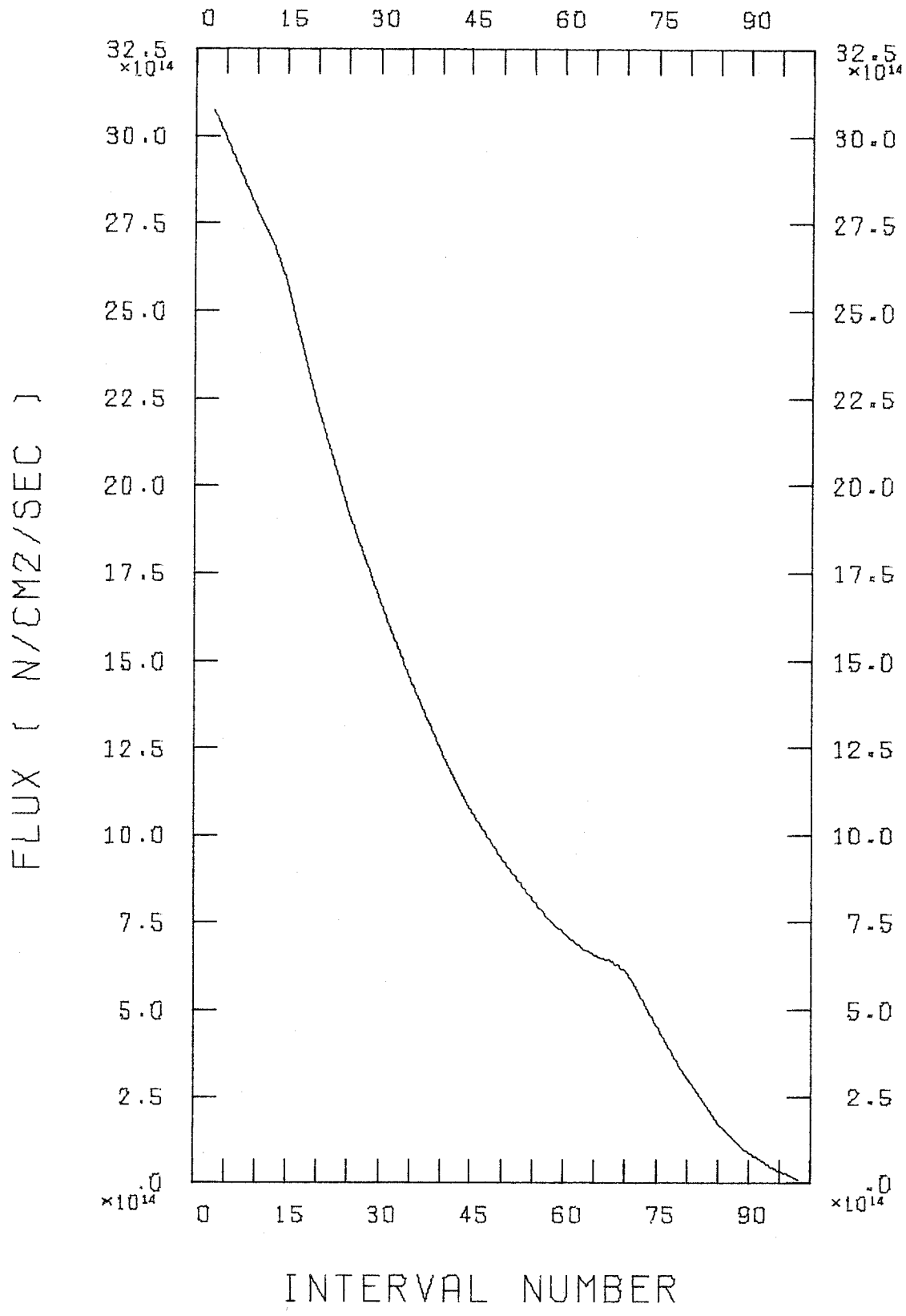

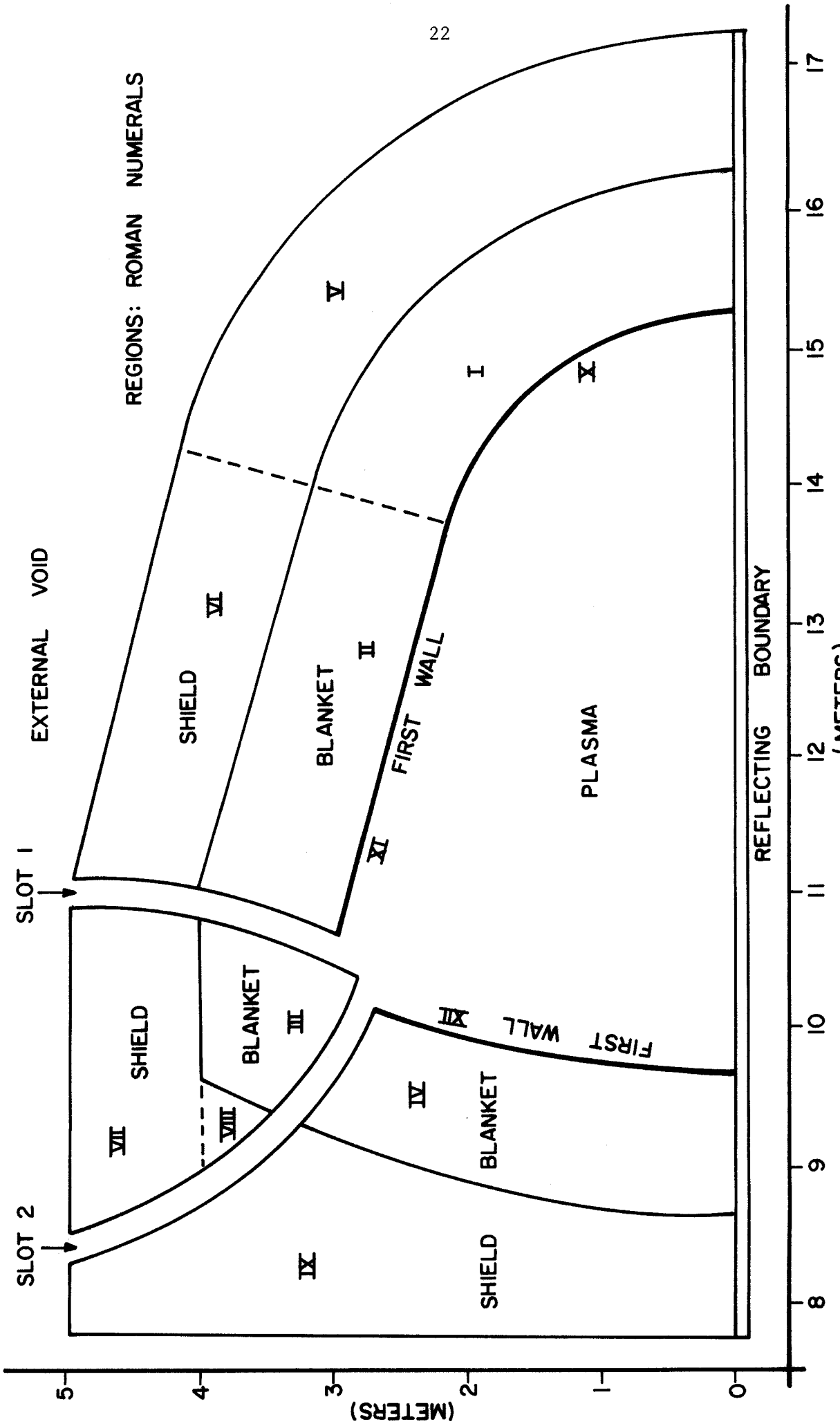

FIG. 5 BLANKET AND SHIELD CONFIGURATION

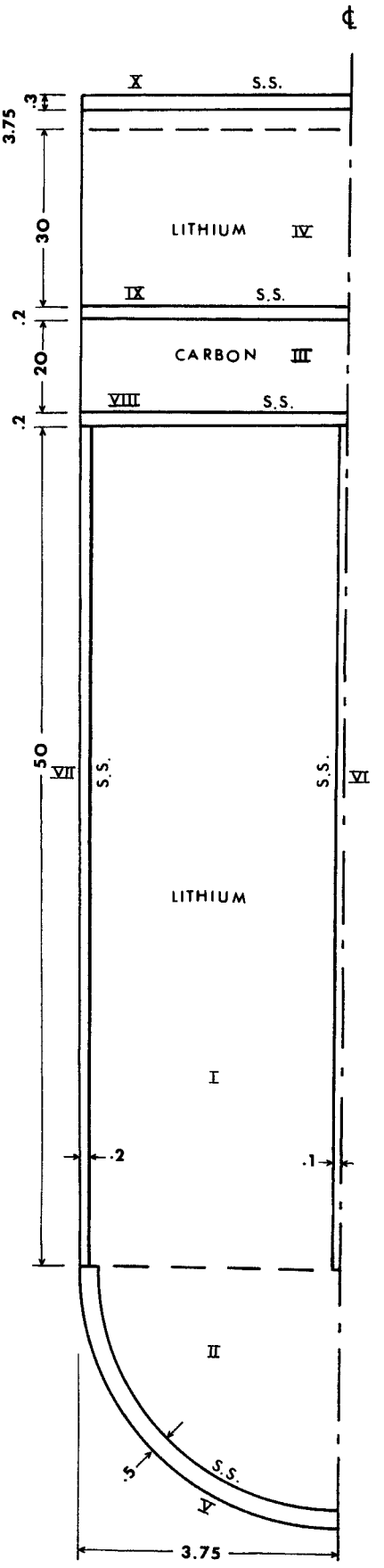

all units are in cm

Regions: Roman Numerals

Figure 6 - Schematic of Unit Cell

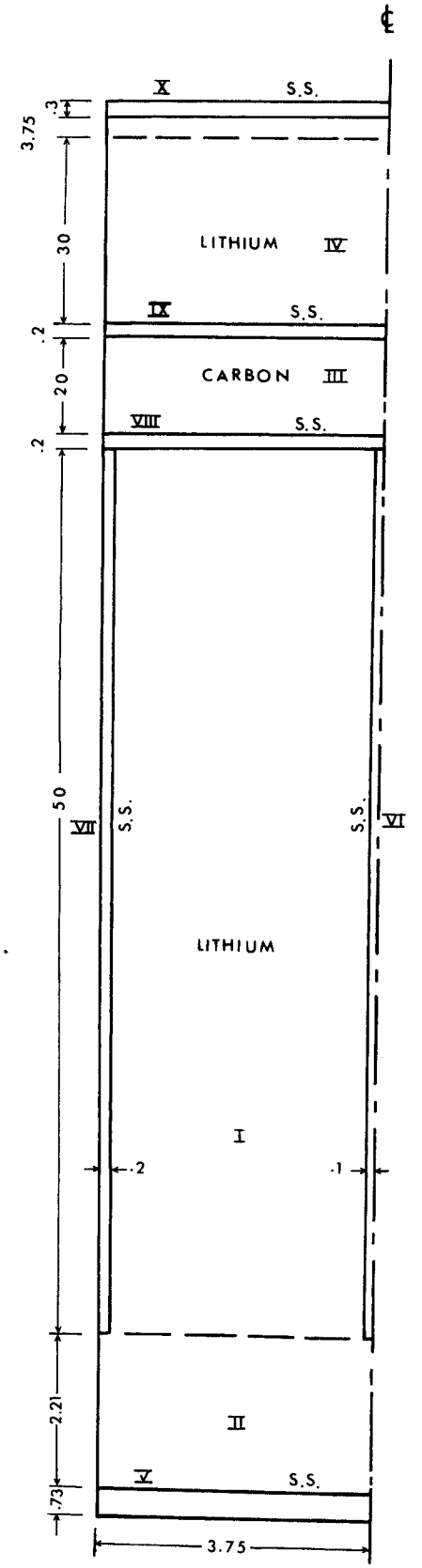

all units are in cm

Regions: Roman Numerals

Figure 7 - Schematic of Unit Cell

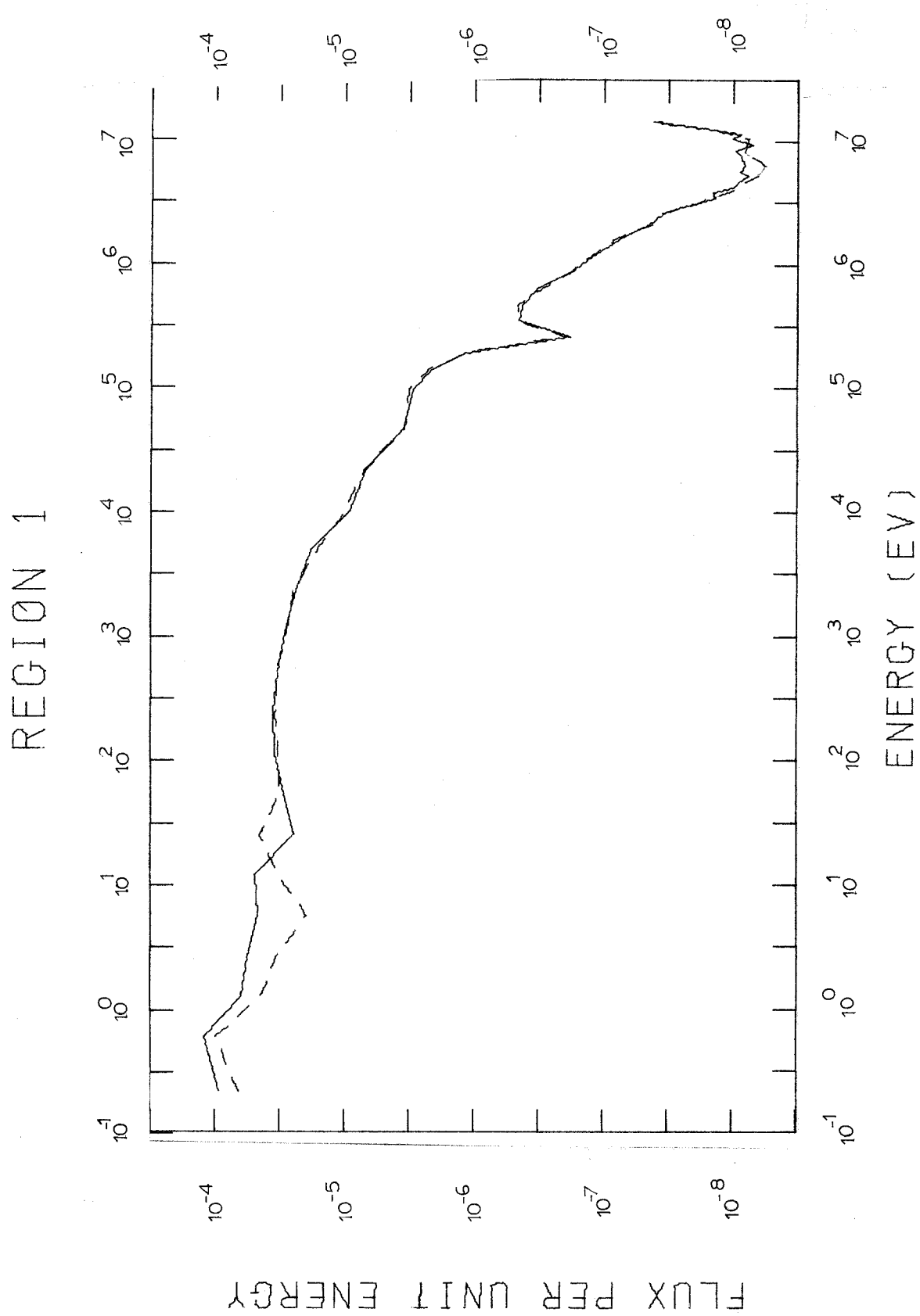

FIGURE 8

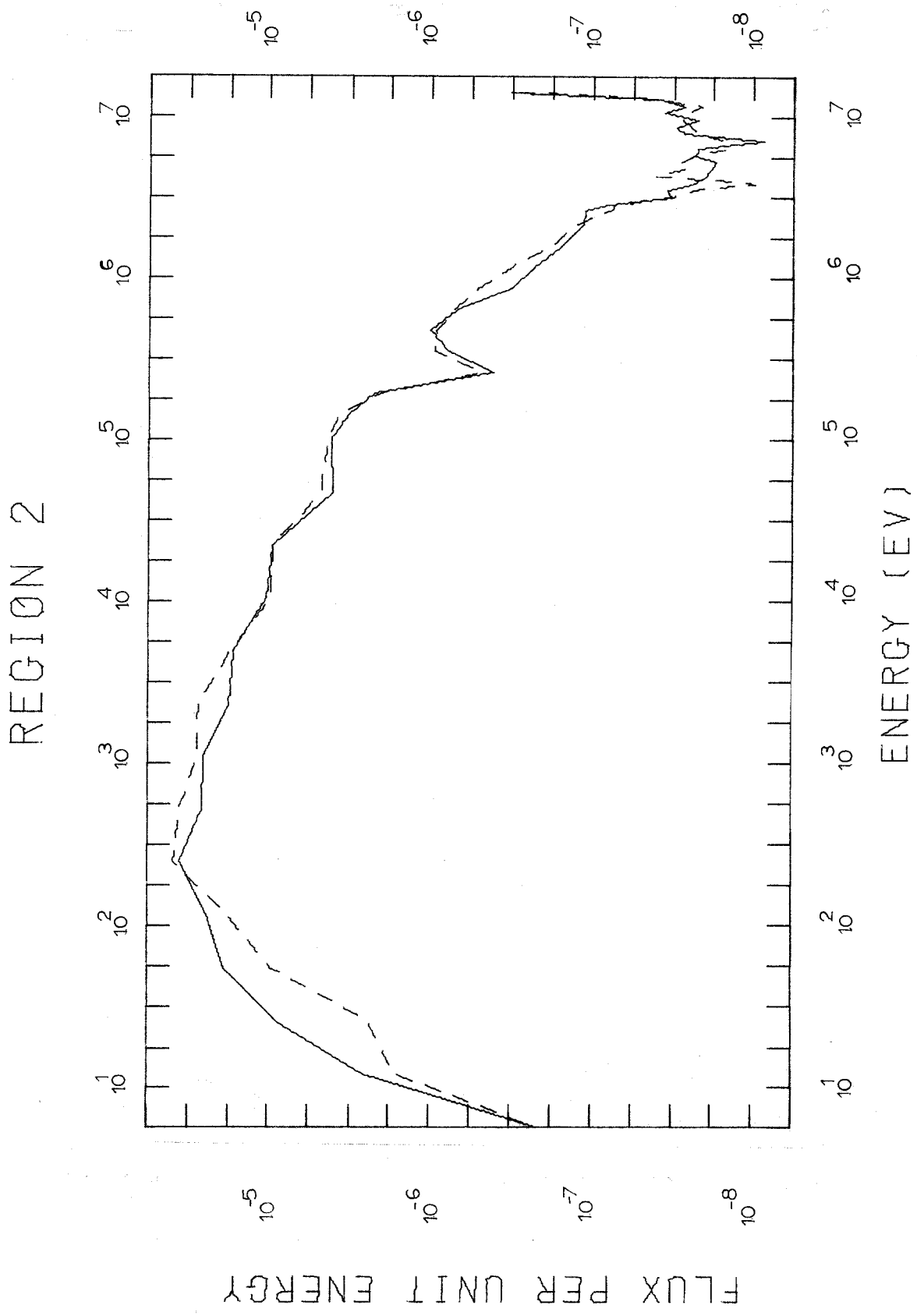
REGION 2
FLUX PER UNIT ENERGY
ENERGY (EV)
10^-5
10^-6
10^-7
10^-8
10^1
10^2
10^3
10^4
10^5
10^6
10^7

FIGURE 9

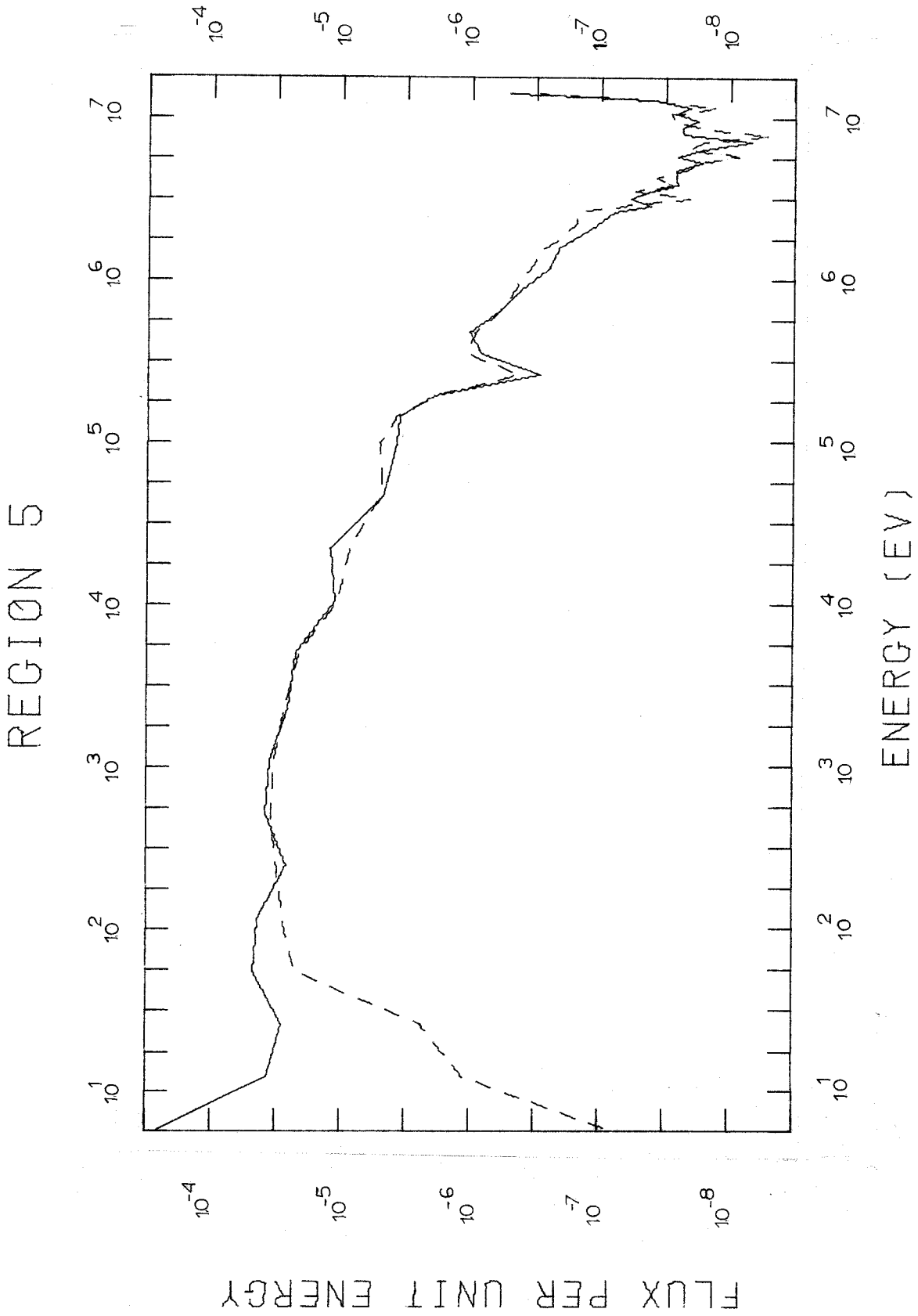

FIGURE 10

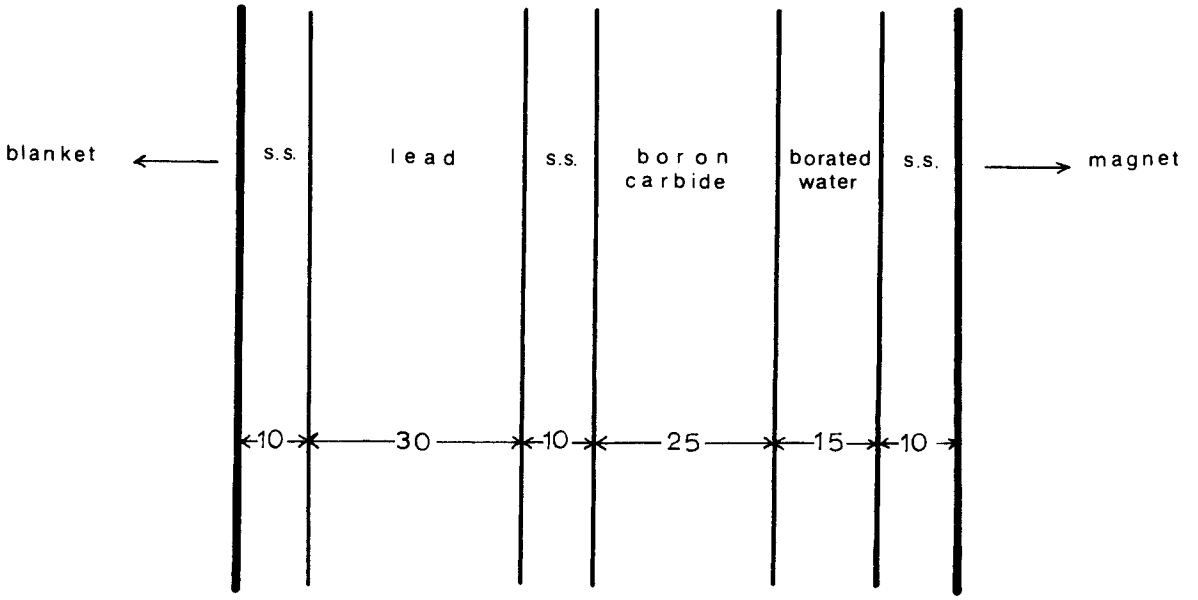

all units are in cm

FIGURE 11- Schematic of Shield

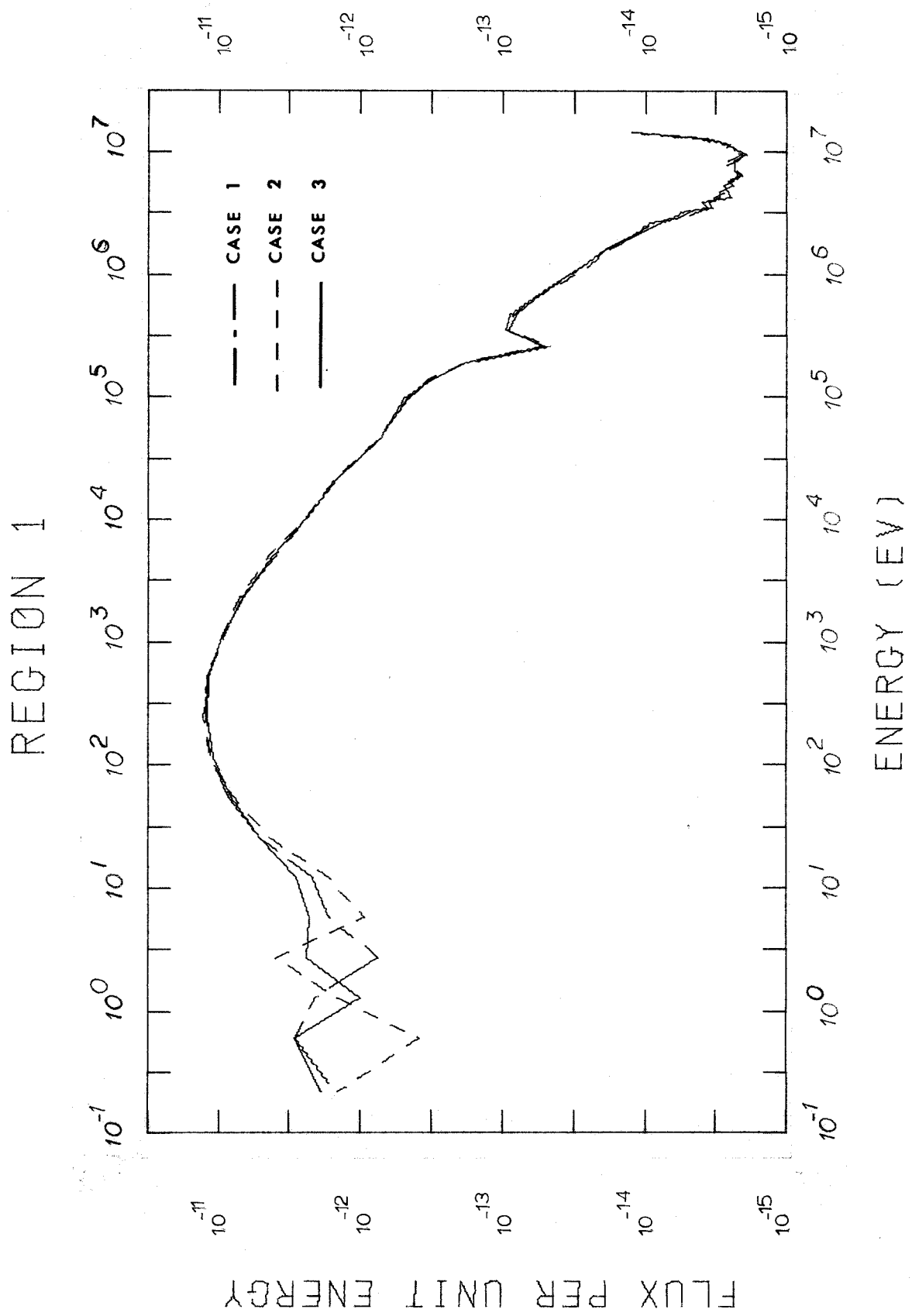

FIGURE 12

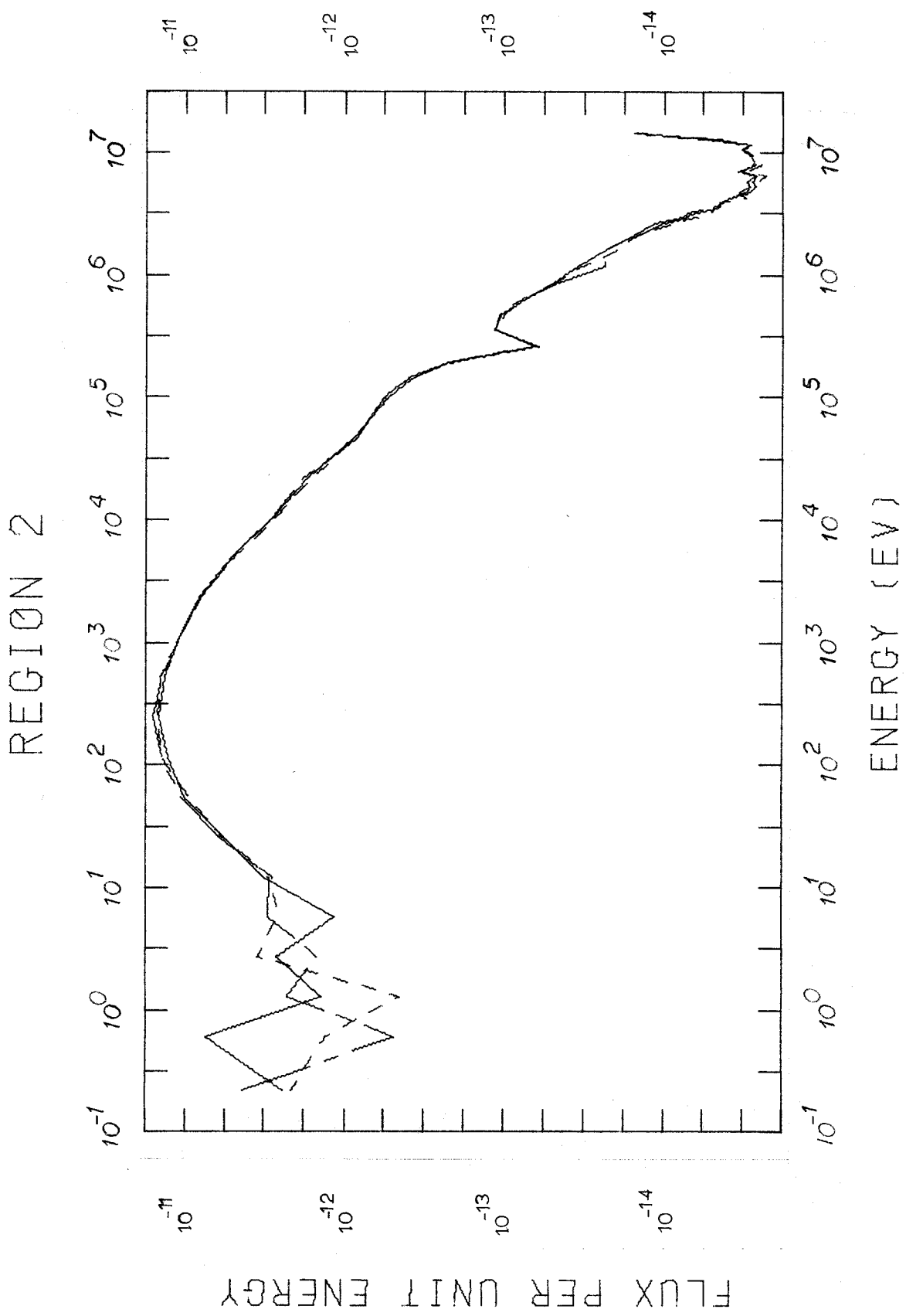
REGION 2
FLUX PER UNIT ENERGY
ENERGY (EV)
10^{-11}
10^{-12}
10^{-13}
10^{-14}
10^{-1}
10^{0}
10^{1}
10^{2}
10^{3}
10^{4}
10^{5}
10^{6}
10^{7}

FIGURE 13

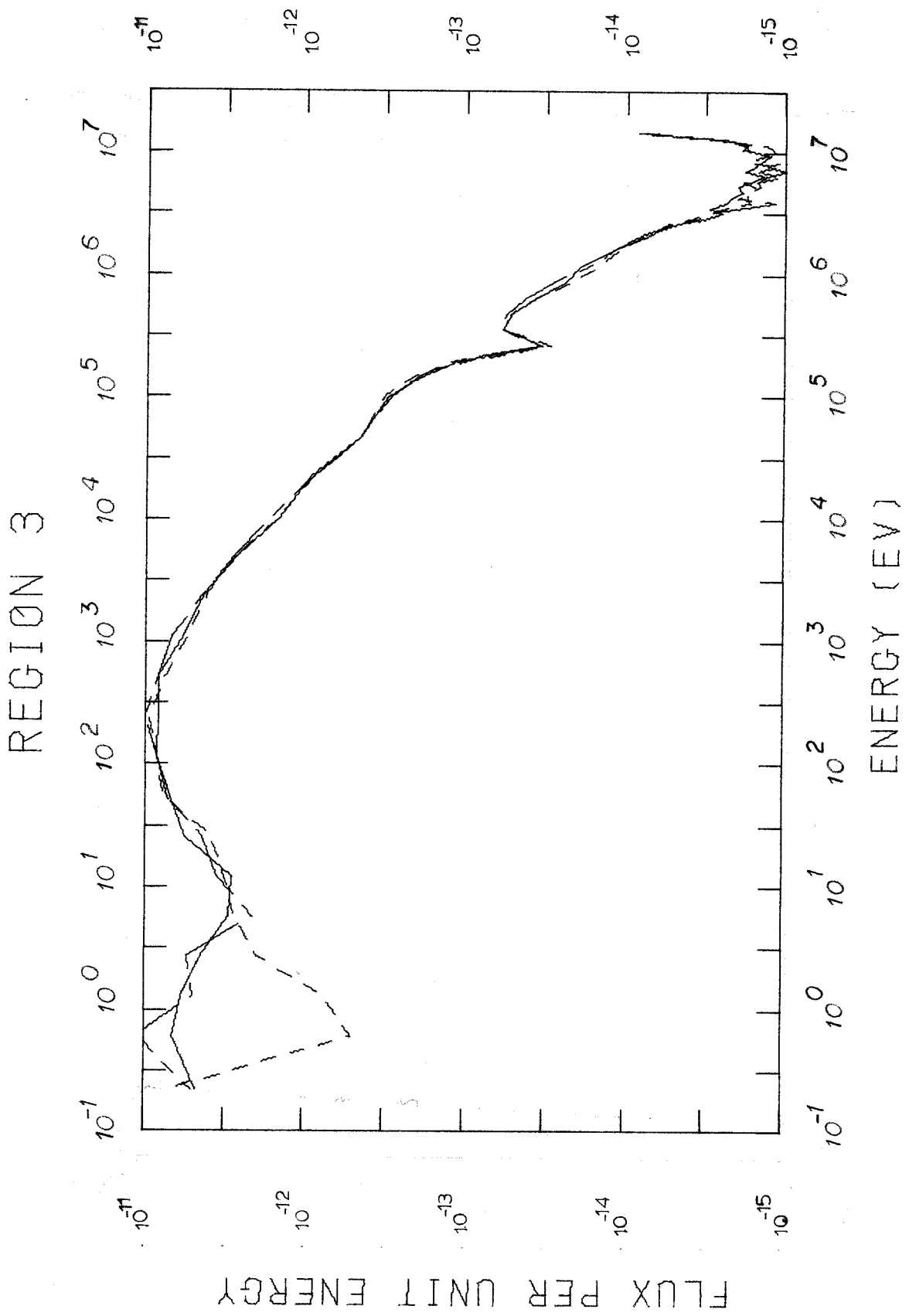

FIGURE 14

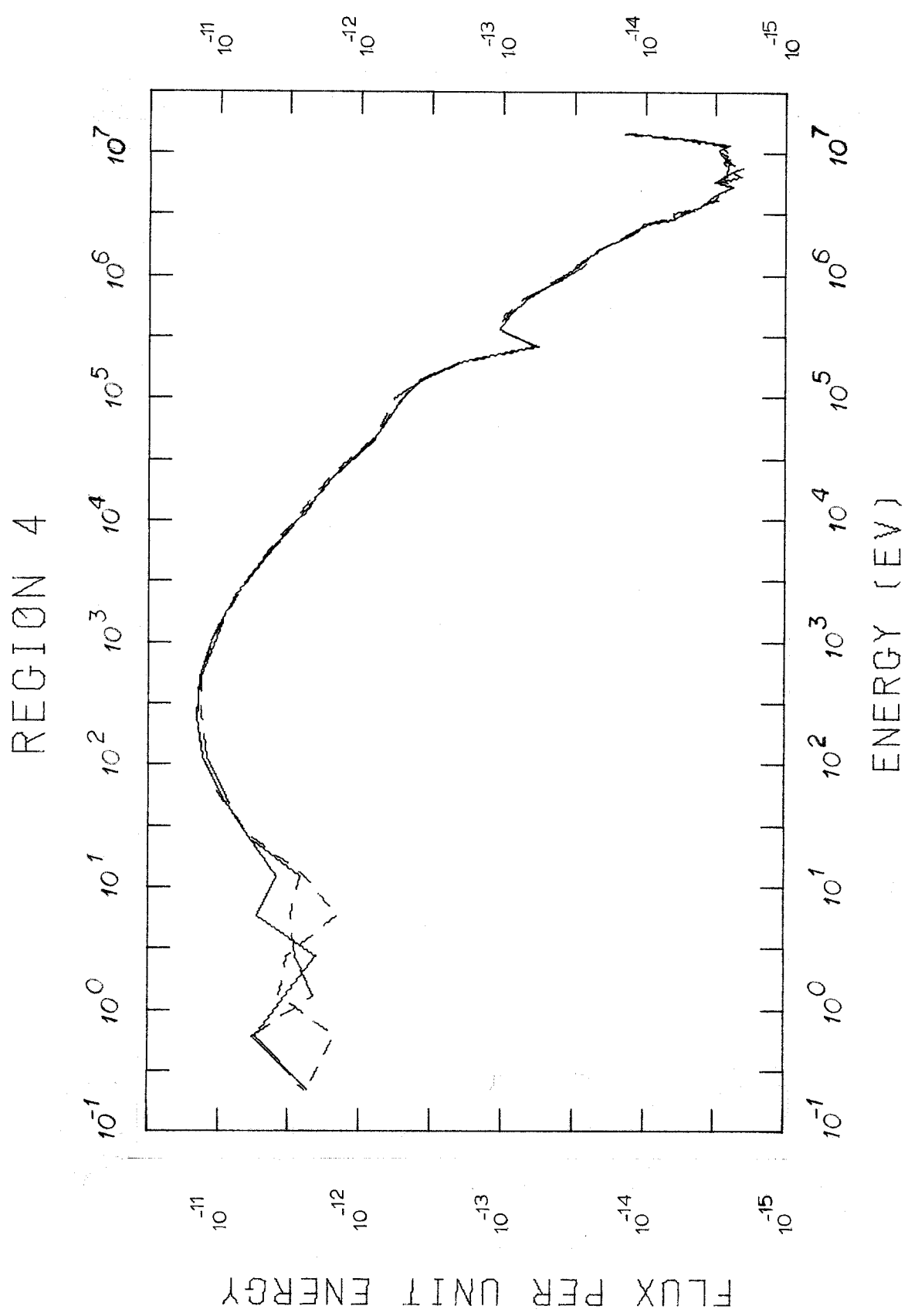

FIGURE 15

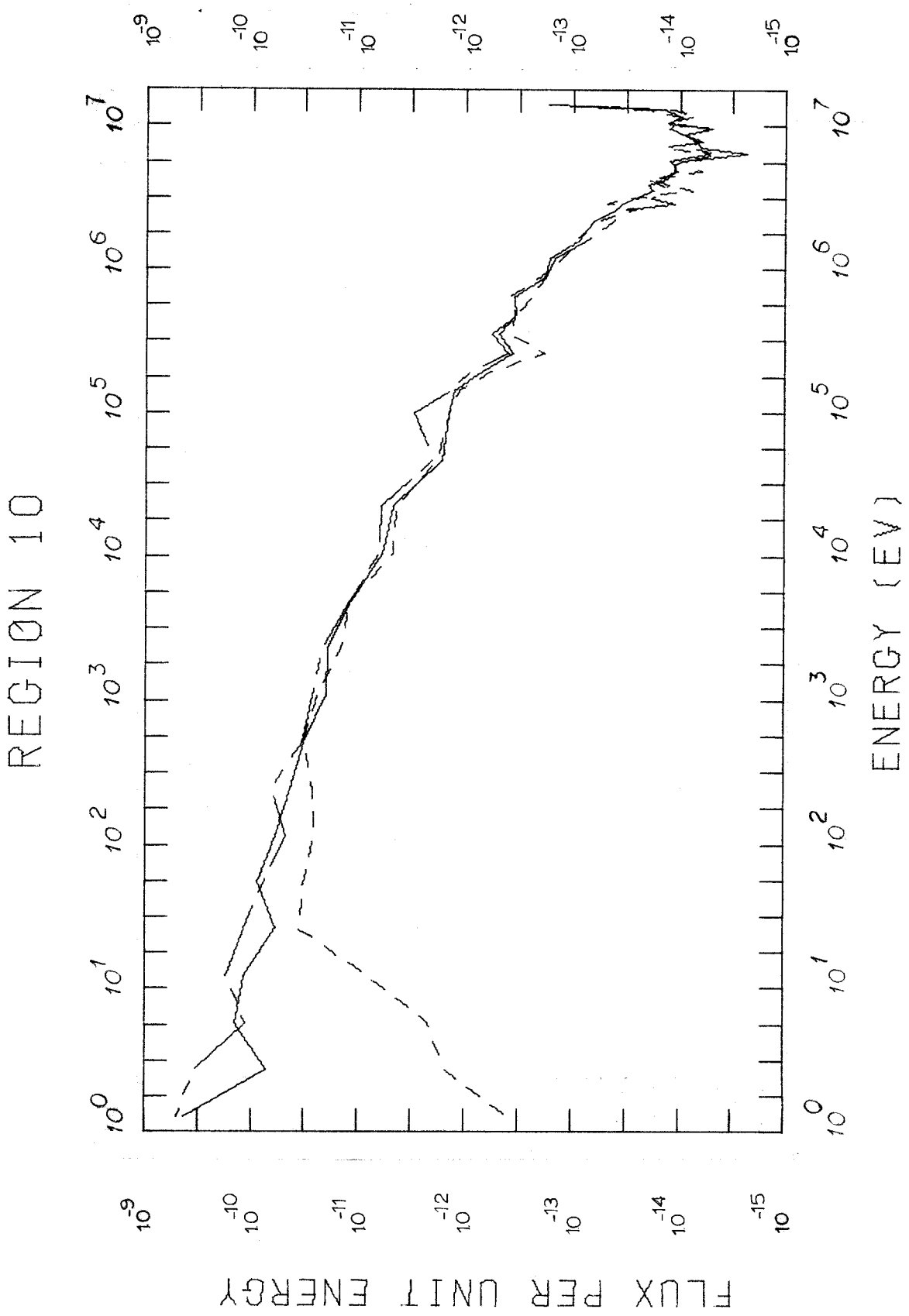

FIGURE 16

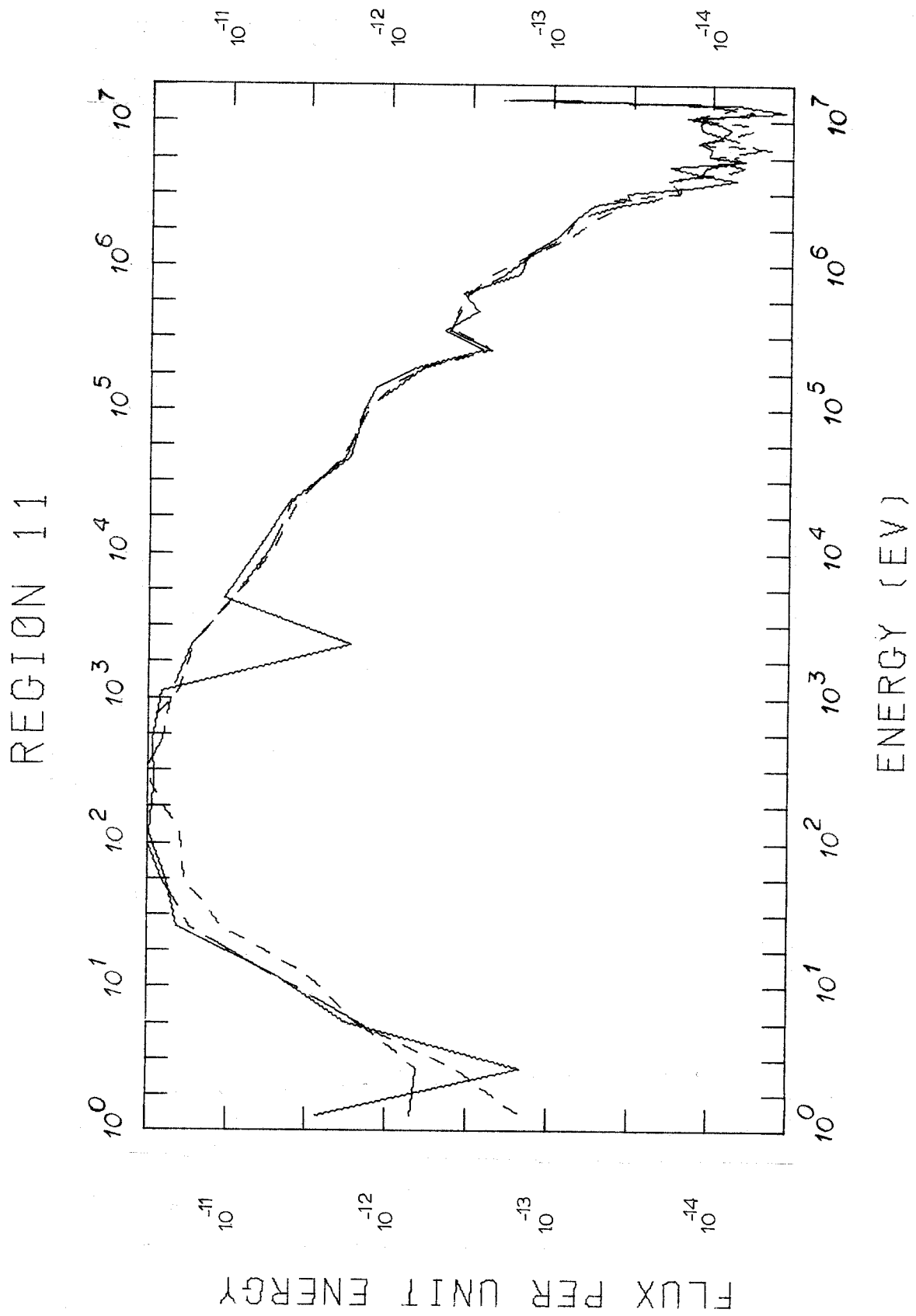
REGION 11
FLUX PER UNIT ENERGY
ENERGY (EV)
10^{-11}
10^{-12}
10^{-13}
10^{-14}
10^{0}
10^{1}
10^{2}
10^{3}
10^{4}
10^{5}
10^{6}
10^{7}

FIGURE 17

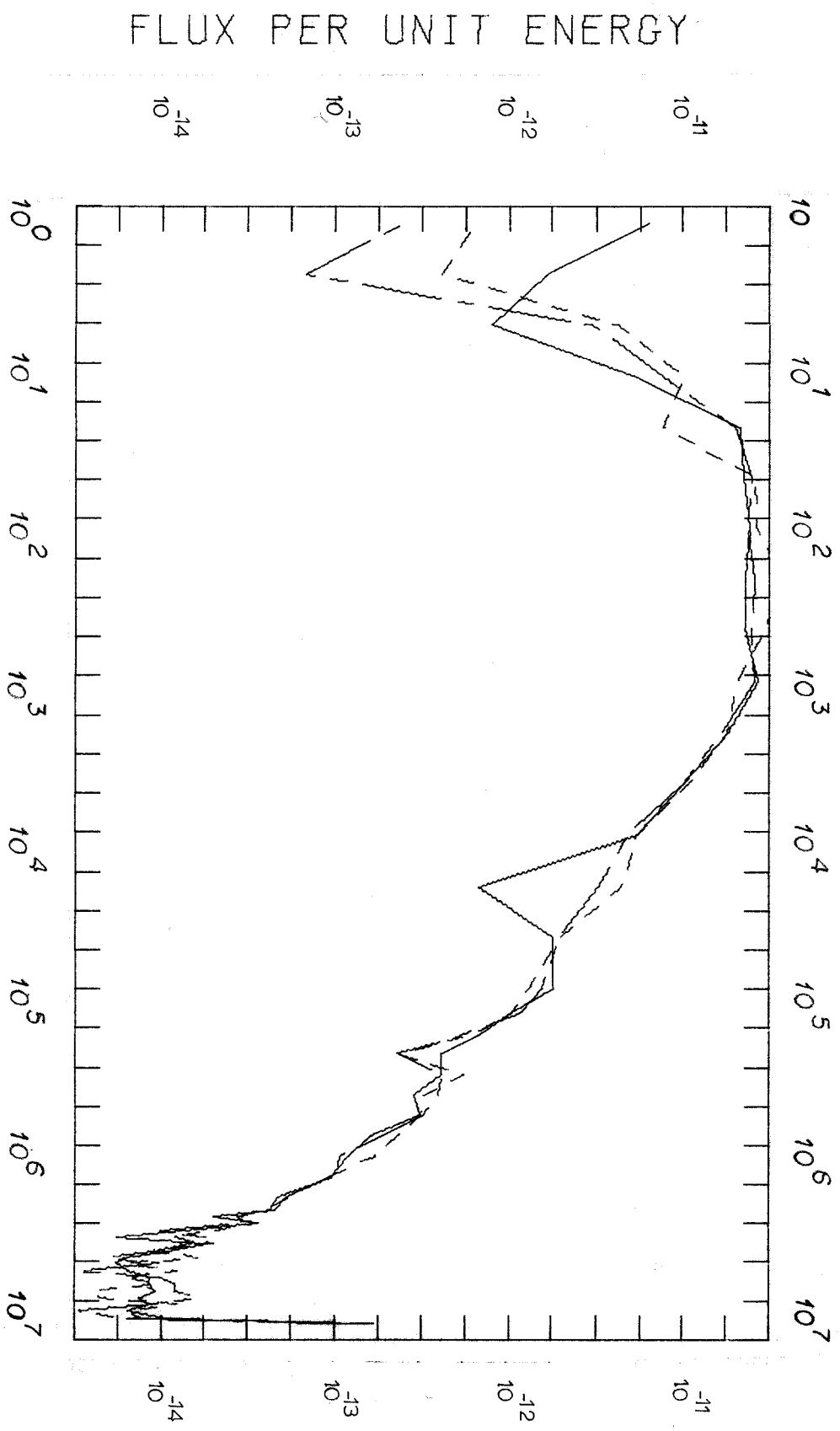
FLUX PER UNIT ENERGY
REGION 12
ENERGY (EV)
10^{-14}
10^{-13}
10^{-12}
10^{-11}
10^{0}
10^{1}
10^{2}
10^{3}
10^{4}
10^{5}
10^{6}
10^{7}

FIGURE 18

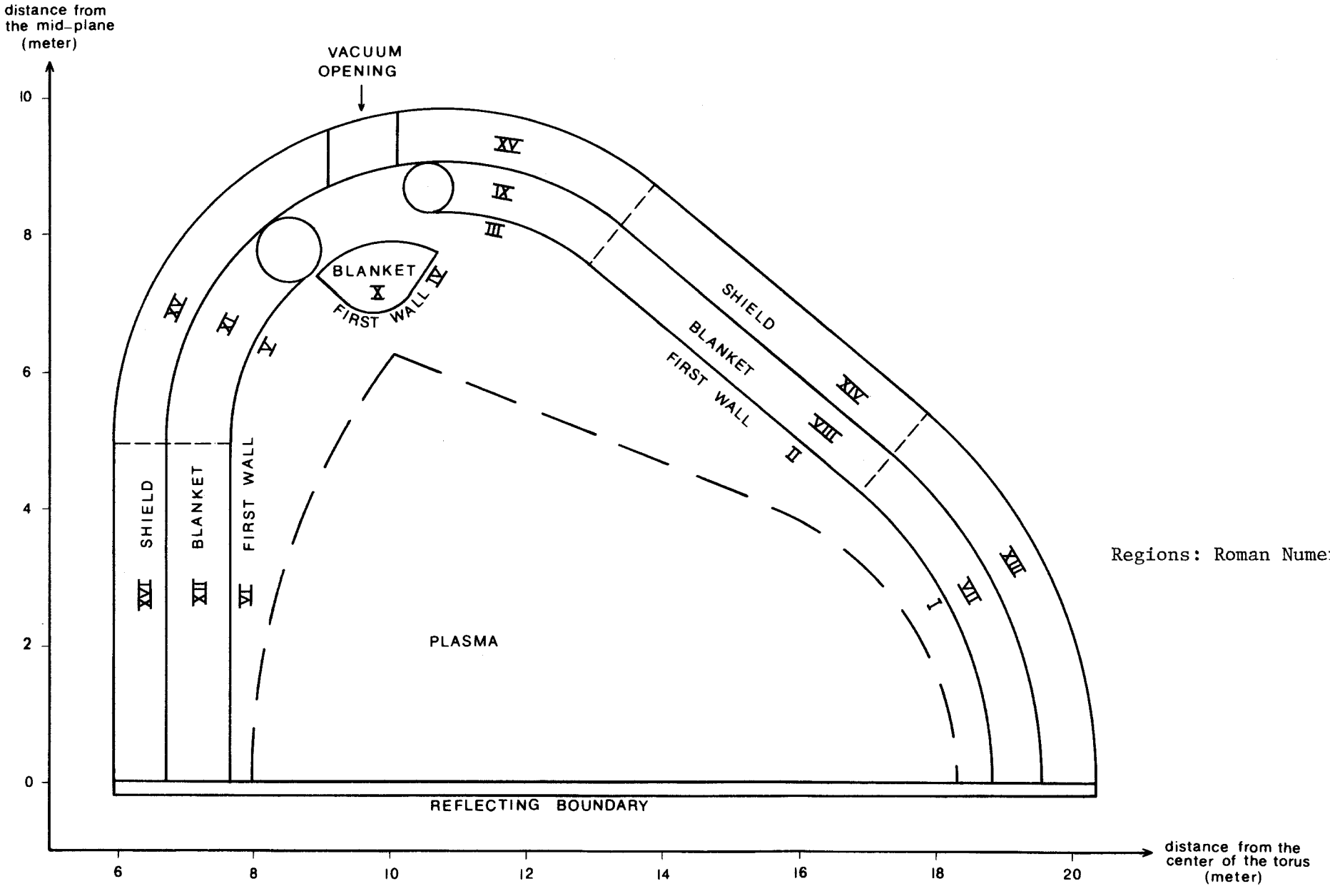

Figure 19 - UWMAK-I Blanket and Shield Configuration

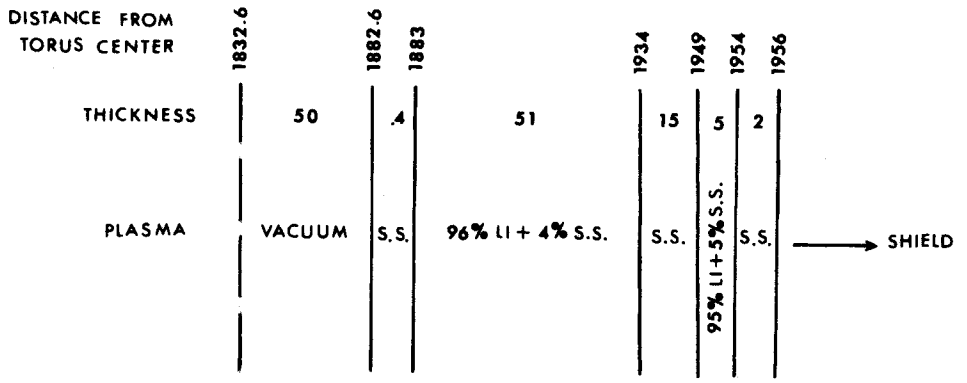

Blanket at left side of plasma

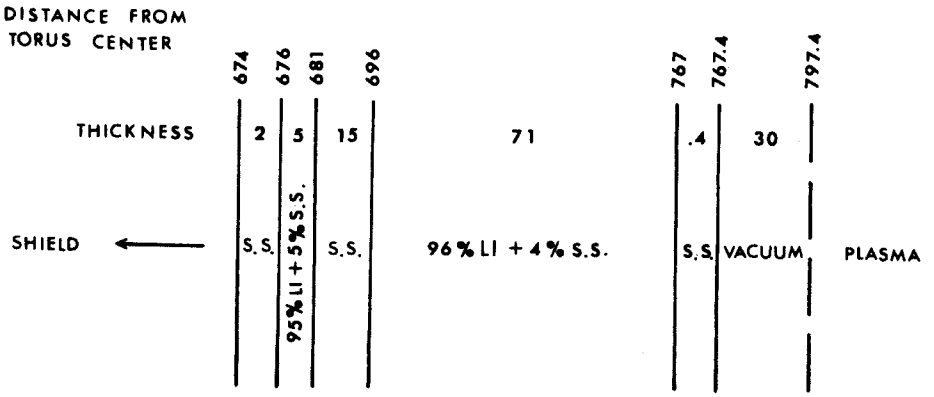

Blanket at Right side of plasma

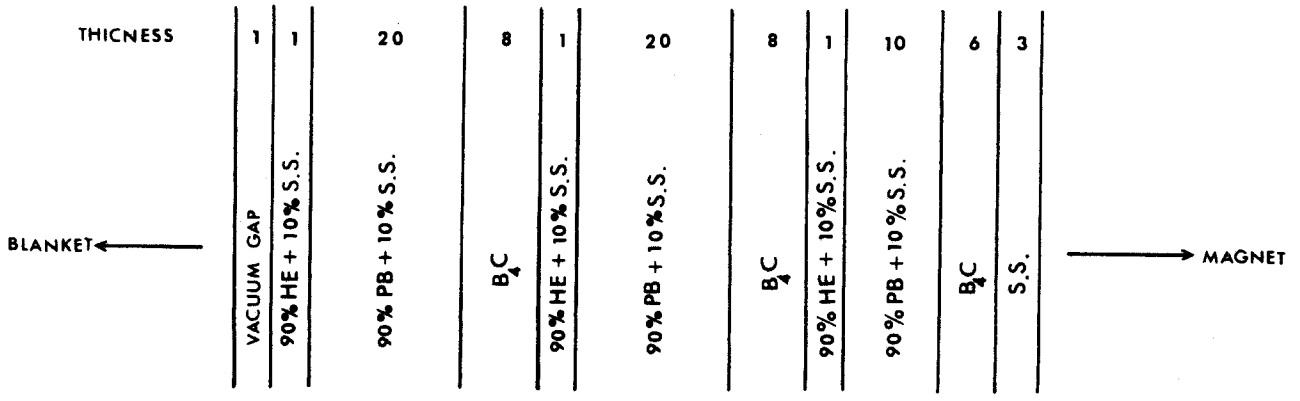

Shield

all units are in cm.

Figure 20 - Schematics of blanket and shield